

Limnol. Oceanogr., 44(2), 1999, 431–435
 © 1999, by the American Society of Limnology and Oceanography, Inc.

Frequency distributions of phytoplankton single-cell fluorescence and vertical mixing in the surface ocean

Abstract—Because of photoacclimation, frequency distributions of phytoplankton single-cell fluorescence reflect variation in light histories among individual cells. As a result, phytoplankton can be used as biological tracers for vertical mixing. A time series of *Prochlorococcus* single-cell fluorescence distributions in the Sargasso Sea revealed changes that were qualitatively consistent with changes in water-column physical dynamics. Applying a photoacclimation-diffusion model to *Prochlorococcus* fluorescence from the time series yields a vertical diffusivity near $30 \text{ cm}^2 \text{ s}^{-1}$ for a remnant mixed layer beneath a diurnal thermocline, which is consistent with estimates obtained by other means. This estimate results from an integrated view of how *Prochlorococcus* responds to changes in light intensity induced by vertical mixing and therefore, may be an appropriate measure of vertical diffusion rates for productivity models that include photoacclimation dynamics. This approach provides a novel way to examine vertical mixing on time scales relevant to phytoplankton physiological responses.

Understanding vertical mixing processes in the surface oceans and consequent phytoplankton photoacclimation has represented a major challenge for oceanographers (Denman and Gargett 1983; Falkowski 1984; Lewis et al. 1984a). This understanding is necessary for interpreting and modeling profiles of primary productivity (e.g., Lewis et al. 1984b; Gallegos and Platt 1985; Mallin and Paerl 1992; Franks and Marra 1994), for predicting the effects of ultraviolet radiation on phytoplankton (Kullenberg 1982; Smith and Baker 1982), and for interpreting ocean color observations. Measurements of average or bulk values of light-sensitive properties of phytoplankton have been used to estimate vertical mixing rates (Falkowski 1983; Lewis et al. 1984a; Theriault et al. 1990); such estimates will be improved by considering properties of individual cells since the within-population distributions of light-sensitive properties contain more information indicative of mixing processes than mean values alone (Lande and Lewis 1989).

We examined the potential to use flow cytometrically (Olson et al. 1993) determined optical properties of the ubiquitous picophytoplankton *Prochlorococcus* as an indicator of mixing processes. *Prochlorococcus* is a small (0.6- μm diameter) and thus effectively neutrally buoyant phytoplankton cell that occurs at densities of 10^4 – 10^5 cells ml^{-1} over large regions of the world's oceans (Chisholm et al. 1988; Olson et al. 1990). Like all phytoplankton, these cells photoacclimate to changing light regimes. Photoacclimation can be observed in situ as changes in single-cell chlorophyll fluorescence, which can be measured using flow cytometry (Olson et al. 1990).

Photoacclimation-diffusion model—Notations used here are defined when first used and are summarized in Table 1.

Prochlorococcus chlorophyll fluorescence (normalized to the 0.33 power of light scatter to remove diel periodicity due to cell growth [Dusenberry 1995]), Γ , and its distribution within a population from a specific depth is determined by both vertical mixing and photoacclimation and can be modeled with a one-dimensional diffusion-photoacclimation equation (Lewis et al. 1984a; Cullen and Lewis 1988) (Fig. 1A):

$$\frac{\partial \Gamma}{\partial t} = \frac{\partial}{\partial z} \left(K_v \frac{\partial \Gamma}{\partial z} \right) + \gamma \Gamma \left(\frac{\Gamma_\infty - \Gamma}{\Gamma_\infty} \right). \quad (1)$$

The first term on the right-hand side parameterizes vertical mixing in terms of a diffusivity, K_v , and the second term represents photoacclimation, modeled using a logistic formulation (Cullen and Lewis 1988), where γ is the photoacclimation rate constant. For chlorophyll fluorescence, the fully acclimated value of single-cell fluorescence, Γ_∞ , is a decreasing function of light intensity; photoacclimation establishes a gradient of increasing fluorescence with depth.

Using a numerical analog to the analytical single-cell model of Lande and Lewis (1989), we have extended the bulk property model of mixing and photoacclimation to a single-cell implementation of Eq. 1. From the individual cell's point of view, Eq. 1 can be rewritten in terms of the cell's normalized fluorescence, Γ , and position, z :

$$\frac{d\Gamma}{dt} = \gamma \Gamma \left(\frac{\Gamma_\infty - \Gamma}{\Gamma_\infty} \right) \quad (2)$$

and

$$\frac{dz}{dt} = \sqrt{2K_v} \xi_t \quad (3)$$

where ξ_t is a “white noise” term used to represent the turbulent vertical movement (sensu Gardiner 1985). To simplify the model, we have assumed K_v to be constant with depth. These equations were combined into a two-dimensional Fokker-Planck equation for the probability density function, N , of cells in Γ and z space:

$$\frac{\partial N}{\partial t} = -\frac{\partial}{\partial \Gamma} \left(N \gamma \Gamma \left[\frac{\Gamma_\infty - \Gamma}{\Gamma_\infty} \right] \right) + K_v \frac{\partial^2 N}{\partial z^2}. \quad (4)$$

Reflective boundary conditions ($\partial N / \partial z = 0$) were imposed at both the surface and base of the mixed layer. For this study, a mixed-layer depth of 70 m was assumed. Both field and laboratory experiments were used to estimate γ ($=3.5 \text{ d}^{-1}$, see below) and Γ_∞ ($=0.5 + 0.2z$, where z is depth in meters) (Dusenberry 1995). Boundary conditions on Γ are such that $N = 0$ for all values of Γ outside the range in Γ_∞ from the surface to the base of the mixed layer. Therefore, $N = 0$ for $\Gamma < 0.5$ and $\Gamma > 14.5$. The integral of N over Γ

Table 1. Summary of notation used.

Symbol	Meaning
γ	Photoacclimation rate constant
Γ	Normalized chlorophyll fluorescence
$\bar{\Gamma}$	Population mean Γ
Γ_∞	Fully acclimated Γ
K_v	Vertical diffusivity
N	Probability density
ξ_r	White noise term
t	Time
z	Depth

was constrained to one at each depth. Related numerical procedures for solution are described fully in Dusenberry (1995). Briefly, an 80×600 (in $\log(\Gamma)$ and z space, respectively) model grid was defined, and a finite-difference approximation for Eq. 4 was created for each node point. The resulting set of linear equations was solved via Gauss-Jordan elimination. Solutions were determined on a log-scaled Γ (64 node points per decade), to correspond directly to flow cytometric data acquisition. We note that this log scaling results in modeled profiles that are not symmetrical with respect to depth (Fig. 1), even though Γ_∞ is linear with depth.

This single-cell approach allows determination of the distribution (including the mean and variance) of Γ within a population of individual cells as a function of depth (Fig. 1). Relatively slow mixing yields frequency distributions with low variances along a gradient in $\bar{\Gamma}$ (the mean value of Γ within the population), as cells have enough time to accli-

mate to their respective light levels (Fig. 1B,C). As diffusivity increases, the gradient in $\bar{\Gamma}$ begins to break down, and at the same time, the distributions of Γ become wider, due to increased variation in light histories (Lande and Lewis 1989) (Fig. 1B,D). Boundary effects also play an important role by reducing variation in both light histories and Γ (Lande and Lewis 1989; Franks and Marra 1994; Kamykowski et al. 1994). As the diffusivity further increases in a bounded mixed layer, $\bar{\Gamma}$ eventually becomes homogeneous with depth. As these rapidly mixed cells photoacclimate to the “average” light intensity they experience, the variation within a population then decreases (Fig. 1B,E). It is important to note that model results reflect only variability that can be attributed to vertical mixing. They do not include “intrinsic” variability from other sources (such as measurement error, genetic variation, etc.). The distribution of Γ on a single-cell basis is thus determined by the vertical diffusivity, the photoacclimation kinetics, and the location of boundaries—namely, the surface and the base of the mixed layer.

Steady-state solutions to this model are discussed more fully in Dusenberry (submitted). A time-dependent model was implemented here. This was identical to the steady-state model, except that the time derivative was approximated using a Crank-Nicholson differencing scheme.

Application to field observations—We applied the time-dependent implementation of the model to a 24-h time series of normalized chlorophyll fluorescence obtained during a cruise to the Sargasso Sea (Fig. 2). Conductivity-tempera-

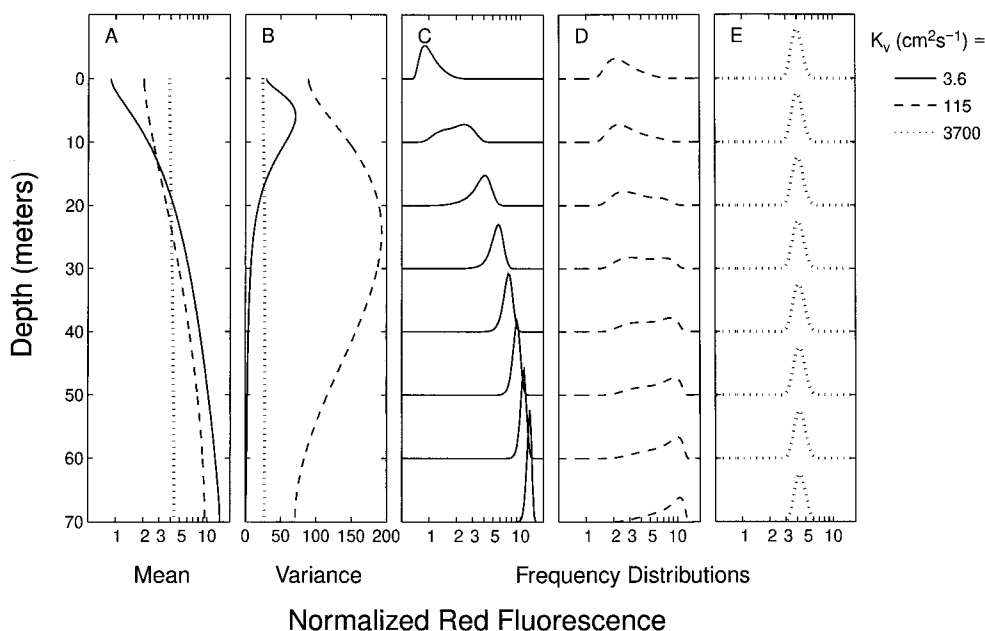


Fig. 1. Numerical solutions (at steady state, with constant K_v) to the model represented by Eq. 1. Results for three different diffusivities ($K_v = 3.6 \text{ cm}^2 \text{ s}^{-1}$, solid lines; $115 \text{ cm}^2 \text{ s}^{-1}$, dashed lines; and $3,700 \text{ cm}^2 \text{ s}^{-1}$, dotted lines) are shown. (A) Mean values ($\bar{\Gamma}$), plotted on a log scale. (B) Variance, calculated on log-scaled results. Results were scaled so that there were 64 data “channels” per decade, and the variances are expressed in units of channels squared. (C–E) Frequency distributions corresponding to the three curves shown in (A) and (B).

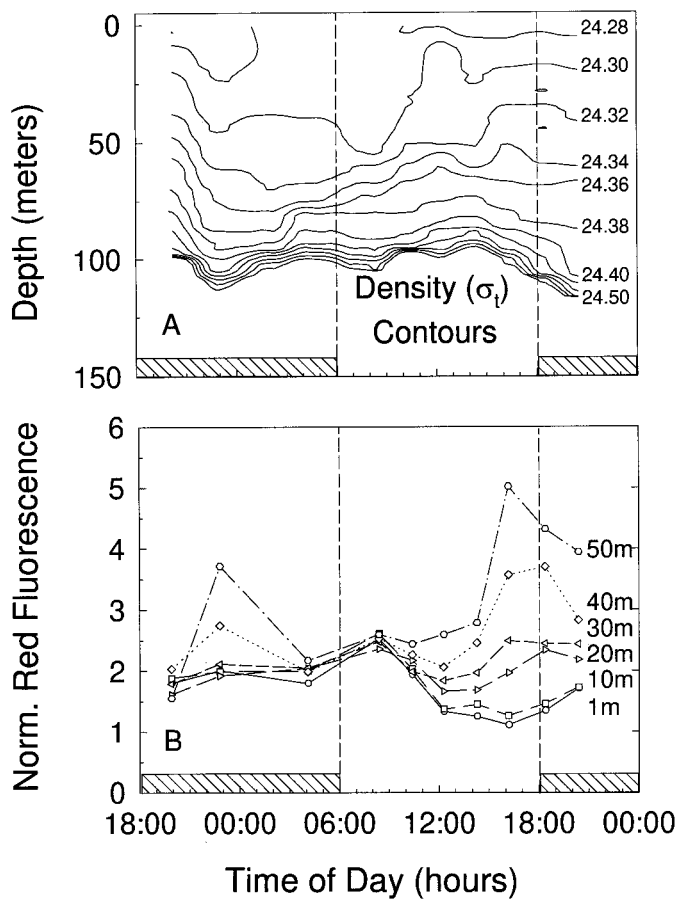


Fig. 2. A 24-h time series of density and the mean of normalized single-cell fluorescence taken at a station in the Sargasso Sea (near 35°25'N, 66°30'W) in October 1989. (A) Density contours. (B) *Prochlorococcus* mean normalized red fluorescence intensity ($\bar{\Gamma}$).

ture-depth (CTD) casts were made, and picophytoplankton samples were collected every 2 h while following a hole-sock drogue set at 25 m. Picophytoplankton samples were preserved for later analysis by fixation with 0.1% glutaraldehyde followed by freezing and storage in liquid nitrogen (Vaulot et al. 1989; Olson et al. 1990). Samples were analyzed using a FACScan flow cytometer; subsequent data were analyzed using a modified version of the CYTOPC software package (D. Vaulot, Station Biologique, Roscoff, France).

Density profiles indicated a shoaling of the mixed layer at midday (Fig. 2A); this is expected to cause a strong reduction in the mixing below a thin surface layer (Price et al. 1986). Flow cytometric measurements revealed that during the day, and particularly after the mixed layer shoaled (around noon), the depth profile of mean *Prochlorococcus* normalized fluorescence ($\bar{\Gamma}$) changed from homogeneous at 0800 h (Fig. 2B) to a strong gradient at 1600 h, suggesting that photoacclimation occurred on a much shorter time scale than vertical mixing.

The effects of mixing can also be seen in the distribution of $\bar{\Gamma}$ within these populations. During the previous night,

mixing within the seasonal mixed layer led to homogeneity in both mean and variance of *Prochlorococcus* normalized fluorescence (Fig. 3A–C). By late afternoon, we expect (based on the steady-state model analysis) both a gradient in mean fluorescence and decreased variance of fluorescence within the populations, especially near the boundaries (e.g., Fig 1C,D). The in situ distributions do show reduction of variances (Fig. 3B,D), except at 20 m, where the relative gradient in mean fluorescence is the largest. This structure in the variance profile suggests that mixing, though slow relative to photoacclimation, is fast enough to have a significant effect on the distributions of *Prochlorococcus* fluorescence.

To estimate vertical mixing rates based on observed distributions of $\bar{\Gamma}$, results from a series of simulations using the time-dependent model with different K_v s were compared to field observations. Measured photoacclimation rates (γ) for normalized single-cell fluorescence range from 1 d⁻¹ to 3.5 d⁻¹ for laboratory and field incubations (Dusenberry 1995). Since field observations (Fig. 2) suggest that in situ rates are more consistent with the higher experimental estimates, we chose to use the highest (3.5 d⁻¹) for this analysis. The model was initialized with observed distributions of $\bar{\Gamma}$ from the 1200-h sampling point (when the mixed layer shoaled). Simulations from 1200 until 1600 h were then completed for a range of vertical diffusivities.

To quantify the goodness of fit between the field observations and predictions of $\bar{\Gamma}$ distributions at a given K_v , the squared residuals between the observed and modeled means and standard deviations were determined for depths corresponding to field observations (Fig. 4). Model results were adjusted by adding 28 channels squared to the variance before the standard deviation was calculated to account for intrinsic variation. An intrinsic coefficient of variation of approximately 19% (unpubl. data) yields a logarithmic equivalent of 28 channels squared on the 64 channels per decade scale used. The area below the minimum contour levels (Fig. 4, crosshatched region) is what we define as the region of best fit. Because modeled population variances are low at both low diffusivities as well as at high diffusivities and the mean value in the interior is relatively insensitive to mixing rates, there appears to be a region of best fit at both low and high diffusivities. However, because the model assumes a constant diffusivity with depth, one needs to evaluate the goodness of fit throughout the water column. The low residuals in the 25–50-m range at high diffusivities do not reflect reasonable fits because of the poor fit near the boundaries.

The best overall agreement for both the mean and standard deviation occurs near a vertical diffusivity of 30 cm² s⁻¹ (Figs. 3D, 4). The deeper depths (30–60 m) show reduced sensitivity to K_v , with best fits obtained at diffusivities 20 cm² s⁻¹ or less, while the best fits at the surface range upward from 30 cm² s⁻¹ to nearly 200 cm² s⁻¹. While we are somewhat constrained in our interpretation because of the assumption of a depth-independent K_v , the results are consistent with larger near-surface diffusivities, decreasing with depth to values on the order of several square centimeters per second. These diffusivities are within the range reported by Denman and Gargett (1983) (mixed-layer K_v s from 0.2 to 80 cm² s⁻¹) and are consistent with vertical diffusivities

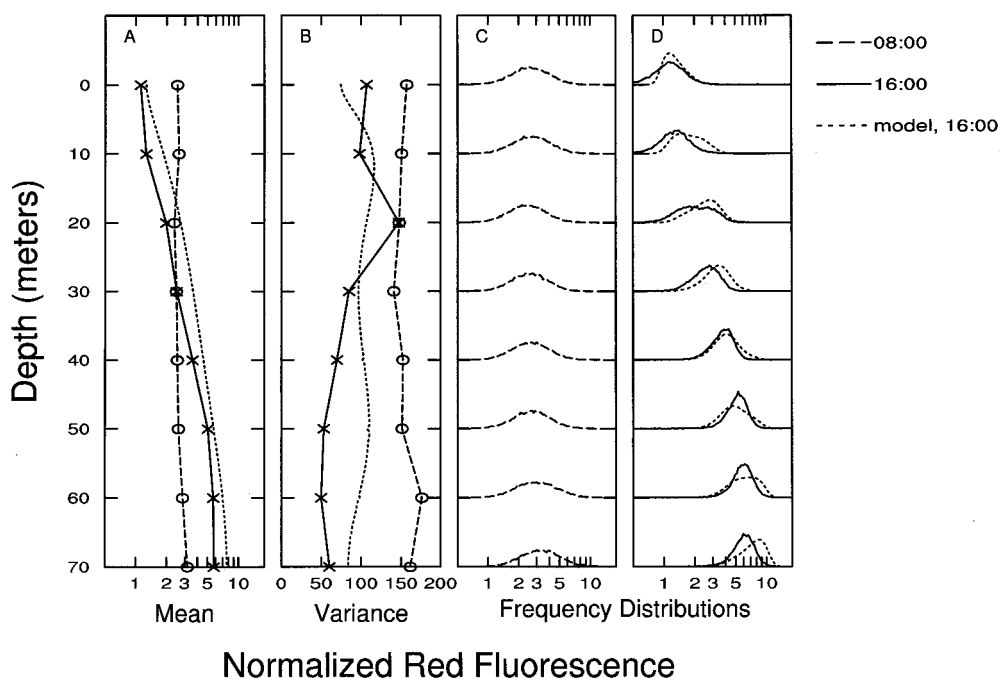


Fig. 3. Profiles from the 0800- and 1600-h time points in the Sargasso Sea time series presented in Fig. 2, plotted on scales corresponding to those used in Fig. 1. (A) Mean normalized *Prochlorococcus* chlorophyll fluorescence. (B) Variance. Units are the same as in Fig. 1. (C–D) Profiles of frequency histograms for the 0800- and 1600-h time points, respectively. The dotted curve in (A), (B), and (D) corresponds to numerical results (at 1600 h) of the time-dependent model (Eq. 1).

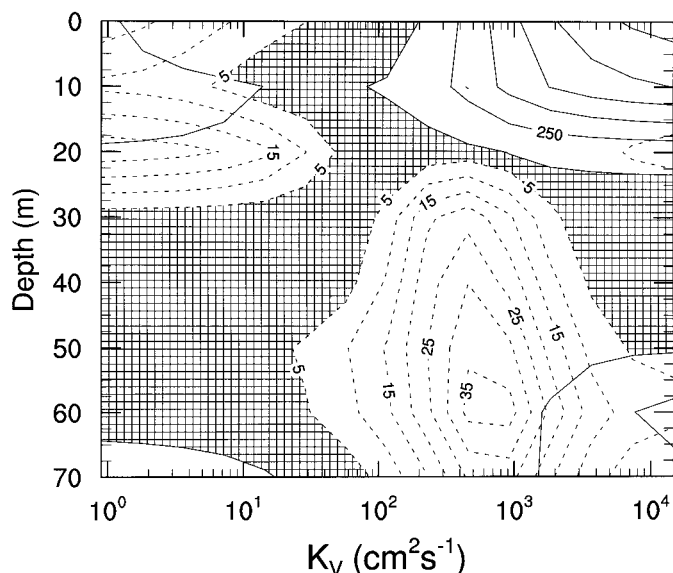


Fig. 4. Contours of the squared residuals between field observations (Fig. 2, 1600 h) and model results as a function of depth and modeled vertical diffusivity. Solid lines represent squared differences between mean values, while dashed lines refer to the squared differences between the standard deviations; units on both sets are channels squared, where the channel is defined as in Fig. 1. The scales on the two sets of contours are different since the squared residuals in the mean had a range more than one order of magnitude larger than that of the standard deviation.

estimated from Brainerd and Gregg's (1993) measurements of turbulent dissipation, ϵ , where $K_v = 0.25\epsilon N^{-2}$ and N is the buoyancy frequency (Denman and Gargett 1983). The vertical diffusivity found here to be consistent with the constant K_v model represents the integrated effects of vertical mixing on the picophytoplankton in the seasonal mixed layer during the 4 h prior to sampling; it most likely reflects the decay of turbulence from the early morning mixed layer (Brainerd and Gregg 1993).

The information about light histories obtained from distributions of photoacclimative properties among individual cells has allowed us to quantify vertical mixing in the upper ocean remnant mixed layer below a shoaled diurnal thermocline. This approach provides a novel way to examine physical mixing processes that occur on time scales relevant to phytoplankton light-induced physiological responses.

Jeffrey A. Dusenberry¹

MIT/WHOI Joint Program in Oceanography
Massachusetts Institute of Technology
Cambridge, Massachusetts 02139

¹ Present address: Division of Engineering and Applied Sciences, Harvard University, Cambridge, Massachusetts 02138.

Acknowledgments

We thank Jim Price for helpful discussions; John Dahlen for the use of the drogue; Trevor Platt for his encouragement; Brian Binder, Raffaella Casotti, Michele DuRand, Sheila Frankel, Lisa Henderson, and Erik Zettler for technical support; and the captain and crew of the RV *Oceanus*. This work received primary support from the Of-

Robert J. Olson

Biology Department
Woods Hole Oceanographic Institution
Woods Hole, Massachusetts 02543

Sallie W. Chisholm²

Department of Civil and Environmental Engineering
Massachusetts Institute of Technology
Cambridge, Massachusetts 02139

References

- BRAINERD, K. E., AND M. C. GREGG. 1993. Diurnal restratification and turbulence in the oceanic surface mixed layer. 1. Observations. *J. Geophys. Res.* **98**: 22645–22656.
- CHISHOLM, S. W., AND OTHERS. 1988. A novel free-living prochlorophyte abundant in the oceanic euphotic zone. *Nature* **334**: 340–343.
- CULLEN, J. J., AND M. R. LEWIS. 1988. The kinetics of algal photoadaptation in the context of vertical mixing. *J. Plankton Res.* **10**: 1039–1063.
- DENMAN, K. L., AND A. E. GARGETT. 1983. Time and space scales of vertical mixing and advection of phytoplankton in the upper ocean. *Limnol. Oceanogr.* **28**: 801–815.
- DUSENBERRY, J. A. 1995. Picophytoplankton photoacclimation and mixing in the surface oceans. Ph.D. thesis, Massachusetts Institute of Technology/Woods Hole Oceanographic Institution.
- FALKOWSKI, P. G. 1983. Light-shade adaptation and vertical mixing of marine phytoplankton: A comparative field study. *J. Mar. Res.* **41**: 215–237.
- . 1984. Physiological responses of phytoplankton to natural light regimes. *J. Plankton Res.* **6**: 295–307.
- FRANKS, P. J. S., AND J. MARRA. 1994. A simple new formulation for phytoplankton photoresponse and an application in a wind-driven mixed-layer model. *Mar. Ecol. Prog. Ser.* **111**: 143–153.
- GALLEGOS, C. L., AND T. PLATT. 1985. Vertical advection of phytoplankton and productivity estimates: A dimensional analysis. *Mar. Ecol. Prog. Ser.* **26**: 125–134.
- GARDINER, C. W. 1985. Handbook of stochastic methods for physics, chemistry, and the natural sciences, 2nd ed. Springer.
- KAMYKOWSKI, D., H. YAMAZAKI, AND G. S. JANOWITZ. 1994. A Lagrangian model of phytoplankton photosynthetic response in the upper mixed layer. *J. Plankton Res.* **16**: 1059–1069.
- KULLENBERG, G. 1982. Note on the role of vertical mixing in relation to effects of UV radiation on the marine environment, p. 283–292. *In* J. Calkins [ed.], The role of solar UV radiation on the marine ecosystems. Plenum.
- LANDE, R., AND M. R. LEWIS. 1989. Models of photoadaptation and photosynthesis by algal cells in a turbulent mixed layer. *Deep-Sea Res.* **36**: 1161–1175.
- LEWIS, M. R., J. J. CULLEN, AND T. PLATT. 1984a. Relationships between vertical mixing and photoadaptation of phytoplankton: Similarity criteria. *Mar. Ecol. Prog. Ser.* **15**: 141–149.
- , E. P. W. HORNE, J. J. CULLEN, N. S. OAKEY, AND T. PLATT. 1984b. Turbulent motions may control phytoplankton photosynthesis in the upper ocean. *Nature* **311**: 49–50.
- MALLIN, M. A., AND H. W. PAERL. 1992. Effects of variable irradiance on phytoplankton productivity in shallow estuaries. *Limnol. Oceanogr.* **37**: 54–62.
- OLSON, R. J., S. W. CHISHOLM, M. ALTABET, E. R. ZETTLER, AND J. A. DUSENBERRY. 1990. Spatial and temporal distributions of prochlorophyte picoplankton in the North Atlantic Ocean. *Deep-Sea Res.* **37**: 1033–1051.
- , E. R. ZETTLER, AND M. D. DURAND. 1993. Phytoplankton analysis using flow cytometry, p. 175–186. *In* P. F. Kemp, B. F. Sherr, E. B. Sherr, and J. J. Cole [eds.], Handbook of methods in aquatic microbial ecology. Lewis.
- PRICE, J. F., R. A. WELLER, AND R. PINKEL. 1986. Diurnal cycling: Observations and models of the upper ocean response to diurnal heating, cooling, and wind mixing. *J. Geophys. Res.* **91**: 8411–8427.
- SMITH, R. C., AND K. S. BAKER. 1982. Assessment of the influence of enhanced UV-B on marine primary productivity, p. 509–537. *In* J. Calkins [ed.], The role of solar UV radiation on the marine ecosystems. Plenum.
- THERRIAULT, J.-C., D. BOOTH, L. LEGENDRE, AND S. DEMERS. 1990. Phytoplankton photoadaptation to vertical excursion as estimated by an *in vivo* fluorescence ratio. *Mar. Ecol. Prog. Ser.* **60**: 97–111.
- VAULOT, D., C. COURTIES, AND F. PARTENSKY. 1989. A simple method to preserve oceanic phytoplankton for flow cytometric analyses. *Cytometry* **10**: 629–635.

Office of Naval Research (grant N00014-87-K-0007), with additional support from the U.S. National Science Foundation. J.A.D. was supported in part by a National Science Foundation Graduate Fellowship.

² To whom correspondence should be addressed.

Received: 20 November 1997

Accepted: 7 November 1998